Adaptive management of excavation-induced ground movements

Richard J. Finno [1)]

[1)] Professor, Department of Civil and Environmental Engineering, Northwestern University, r-finno@northwestern,edu

SYNOPSIS: This paper describes an adaptive management approach for predicting, monitoring, and controlling ground movements associated with excavations in urban areas. Successful use of monitoring data to update performance predictions of supported excavations depends equally on reasonable numerical simulations of performance, the type of monitoring data used as observations, and the optimization techniques used to minimize the difference between predictions and observed performance. This paper summarizes each of these factors and emphasizes their inter-dependence. Numerical considerations are described, including the initial stress and boundary conditions, the importance of reasonable representation of the construction process, and factors affecting the selection of the constitutive model. Monitoring data that can be used in conjunction with current numerical capabilities are discussed, including laser scanning and webcams for developing an accurate record of construction activities, and automated and remote instrumentations to measure movements. Self-updating numerical models that have been successfully used to compute anticipated ground movements, update predictions of field observations and to learn from field observations are summarized. Applications of these techniques from case studies are presented to illustrate the capabilities of this approach.

Key Words: Supported excavations, finite element, field performance, inverse analysis, clays

1. Introduction

With new development, and increasingly more redevelopment, within urban areas there is a clear need to efficiently and safely develop underground space. A major concern when placing deep excavations in urban environments is the impact of construction-related ground movements on adjacent buildings and utilities. In practice, when designers are faced with an excavation where ground movements are a critical issue, they can estimate movements using semi-empirical methods or results of numerical modeling. While numerical simulations have become more common to analyze ground response to excavations as part of the design process, finite element predictions contain uncertainties related to soil properties, support system details, and construction procedures. If one wants to predict and subsequently evaluate the overall performance of a design, a procedure that incorporates an evaluation of the results of the predictive analysis must be defined. The procedure to accomplish this task is usually referred to as the "observational method" (Peck, 1969), a framework wherein construction and design procedures and details are adjusted based upon observations and measurements made as construction proceeds. While the observational method is conceptually very helpful, it is quite difficult to use observed movements for controlling construction in a timely enough fashion to be of use in a typical excavation project, where time is of the essence to a contractor, or to judge quantitatively how well the work is proceeding.

While it is common to include a monitoring program during construction to record the ground movements, structural responses of the support system, and, in some cases, adjacent building movements, it is rare that these observations are used to control the construction process and update predictions of movements given the measured deformations at early stages of construction. Whereas significant developments have been made in the acquisition of field data, efforts to integrate various components of data acquisition and prediction of deformations have had limited success due to difficulty of the problem and the presence of several missing links to complete the deformation construction cycle. Furthermore, many factors affect the ground movements caused by excavations,

including stratigraphy, soil properties, support system details, construction activities, contractual arrangements and workmanship.

This paper describes an adaptive management approach to predict, monitor, and control ground movements associated with excavations in urban areas. The goal of this approach is to allow one to use the observed performance at early stages of a project to objectively calibrate a predictive model so that reliable predictions of subsequent performance can be made. The successful application of such techniques depends on the predictive model, in this case a finite element simulation of construction, the monitoring data and the inverse technique itself. This paper will illustrate these points by examining the technique as applied to supported excavations made through soft to medium clays. Comments are made regarding how details of the finite element simulations, the instrumentation and data collection, and the inverse technique affect the results of the methodology. Several examples of excavations where these techniques were applied are presented.

2. Finite Element Predictions of Excavation Performance

A key to a successful finite element simulation is to reasonably represent within a numerical simulation pertinent field activities during construction. In addition to replicating construction procedures and dimensionality of the problem, one must also carefully consider the applicability of a constitutive model to replicate the aspects of behavior that most affect the measurements that one makes to evaluate performance.

2.1 Representing Field Conditions in Finite Element Simulations

While supported excavations commonly are simulated numerically by modeling stages of excavation and support installation, it is necessary to simulate all aspects of the construction process that affect the stress conditions around the excavation to obtain an accurate prediction of behavior. This may involve simulating previous construction activities at the site, installation of the supporting wall and any deep foundation elements, as well as the removal of cross-lot supports or detensioning of tiedback ground anchors. Furthermore, issues of time effects caused by hydrodynamic effects or material responses may be important.

Finno and Tu (2006) summarized the effects of a number of key numerical assumptions on the computed performance of supported excavations. The manner in which the excavation is simulated including the removal of soil elements in a finite elements mesh should satisfy the principal of superposition as described by Ghaboussi and Pecknold (1985). Other key assumptions include selecting appropriate drainage conditions during excavation (Clough and Mana 1976; O'Rourke and O'Donnell 1997; Whittle et al. 1993), starting with appropriate initial effective stresses that include the effects of past construction activities at a site (Calvello and Finno 2003), and accurately defining the initial ground water conditions for a site (e.g. Finno et al. 1989). Many times the effects of the installation of a wall are ignored in a finite element simulation and the wall is "wished-into-place" with no change in the stress conditions in the ground or any attendant ground movements. However, there is abundant information (e.g. Clough et al. 1989; O'Rourke and Clough 1990; Finno et al. 1988; Sabatini 1991; Koutsoftas et al. 2000) that shows ground movements may arise during installation of the wall, and, if ignored, these may have a significant impact on the accuracy of the computed responses, particularly in cases where the resulting ground deformations are relatively small. One must take care when representing the bracing system in a model. In typical plane strain simulations, application of prestress for cross-lot braces and installation of tiedback ground anchors can present problems under certain circumstances (e.g. Finno and Tu 2006).

Even with properly defined initial conditions, challenges remain. Figure 1 illustrates some of the challenges of using field observations to calibrate numerical models of any kind, even when detailed records exist. This figure summarizes the construction progress at the Chicago-State excavation (Finno et al 2002) in terms of excavation surface and support installation on one of the walls of the excavation for selected days after construction started. Also shown are the locations of two inclinometers placed several meters behind the wall. If one is making a computation assuming plane strain conditions, then it is clear that one must judiciously select a data set so that

planar conditions would be applicable to a set of inclinometer data. If one is using an adaptive management approach wherein data is collected and compared with numerical predictions in almost real time, then it is clear that a 3D analysis would be required for most days as a result of the uneven excavated surface and timing of the anchor prestressing operations.

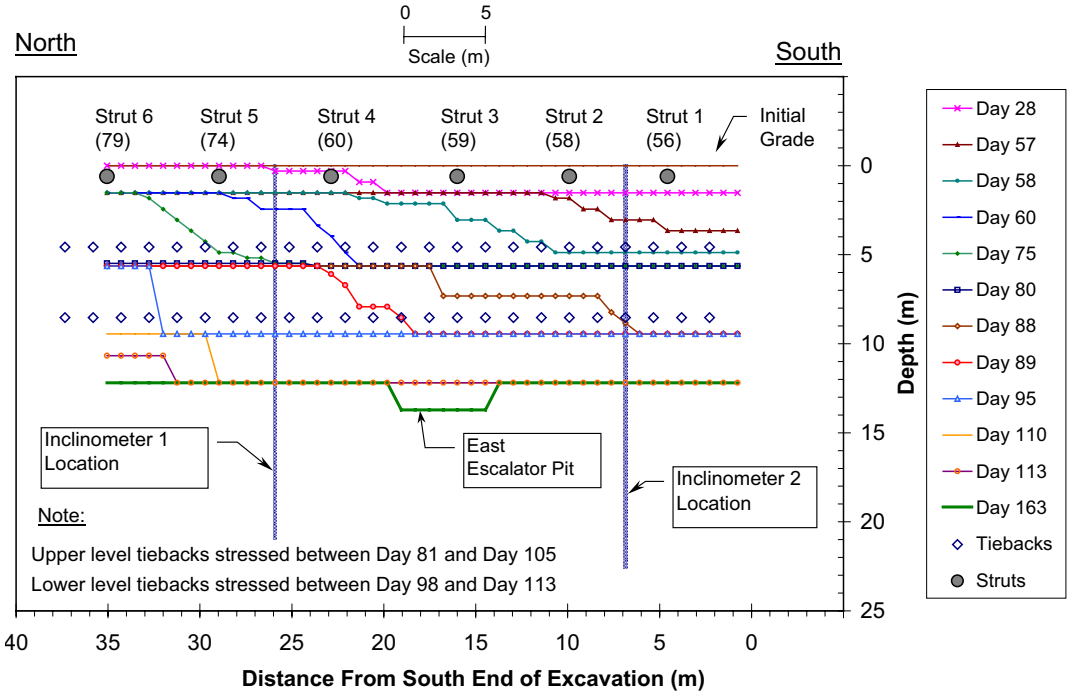

Figure 1. Construction progress at excavation in Chicago (Finno et al 2002)

Even when a sufficiently extensive horizontal excavated surface is identified, 3-dimensional effects may still arise from the higher stiffness at the corners of an excavation. These boundary conditions lead to smaller ground movements near the corners and larger ground movements towards the middle of the excavation wall. Another, and less recognized, consequence of the corner stiffening effects is the maximum movement near the center of an excavation wall may not correspond to that found from a conventional plane strain simulation of the excavation, i.e., 3-dimensional (3-D) and plane strain simulations of the excavation do not yield the same movement at the center portion of the excavation, even if the movements in the center are perpendicular to the wall (Ou et al. 1996). Finno et al. (2007) quantified this effect by the plane strain ratio, PSR, defined as the maximum movement in the center of an excavation wall computed by 3-D analyses divided by that computed by a plane strain simulation. As shown in Figure 2, a key indicator is the L/H_e ratio, where L is the dimension of the excavation where the movement occurs, and H_e is the excavation depth. When L/H_e is greater than 6, the PSR is equal to 1 and results of plane strain simulations yield the same displacements in the center of an excavation as those computed by a 3-D simulation. When L/H_e is less than 6, the displacement computed from the results of a plane strain analysis will be larger than that from a 3-D analysis. When conducting an inverse analysis of an excavation with a plane strain simulation, the effects of this corner stiffening is that an optimized stiffness parameter will be larger than it really is because of the lack of the corner stiffening in the plane strain analysis. This effect becomes greater as an excavation is deepened because the L/H_e value increases as the excavated grade is lowered. This trend was observed in the optimized parameters for the deeper strata at the Chicago-State subway renovation excavation (Finno and Calvello 2005).

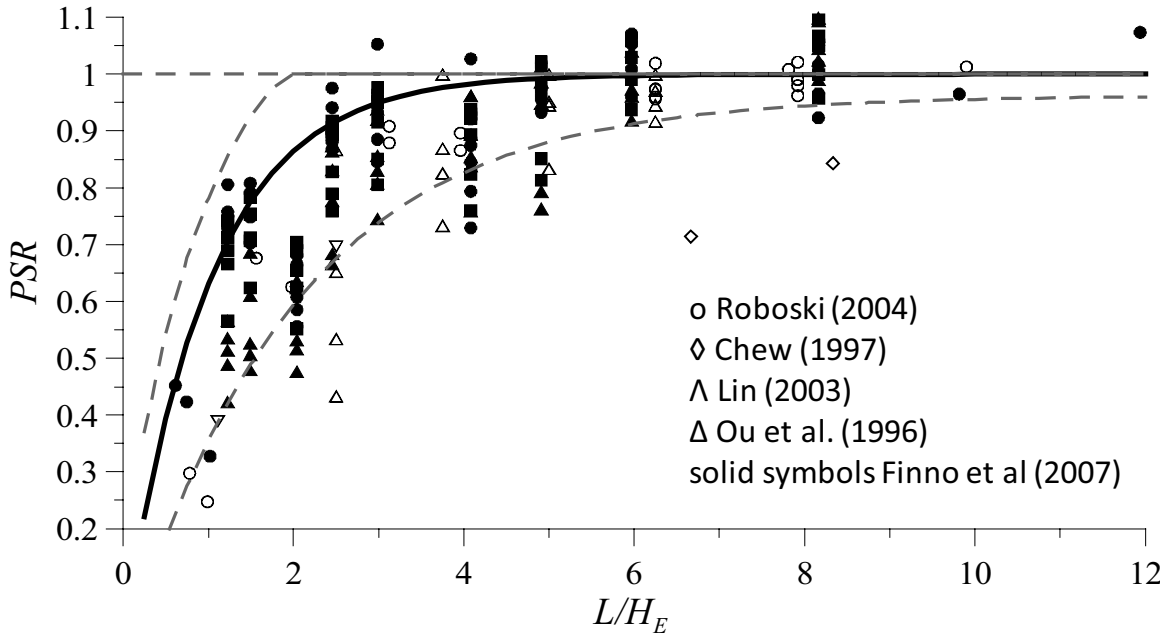

Figure 2. Effects of geometry on 3-D movements of excavations

2.2 Soil Constitutive Behavior

When one undertakes a numerical simulation of a deep supported excavation, one of the key decisions made early in the process is the selection of the material constitutive models representing the various soil formations at the site. If the results form the basis of a prediction that will be updated based on field performance data, then the types of field data that form the basis of the comparison will impact the applicability of a particular model. Possibilities include lateral movements based on inclinometers, vertical movements at various depths and distances from an excavation wall and/or forces in structural support elements. When used for a case where control of ground movements is a key design consideration, the constitutive model must be able to reproduce the soil response at appropriate strain levels to the imposed loadings.

It is useful to recognize that soil is an incrementally nonlinear material, i.e., its stiffness depends on loading direction and strain level. Soils are neither linear elastic nor elasto-plastic, but exhibit complex behavior characterized by zones of high constant stiffness at very small strains, followed by decreasing stiffness with increasing strain. This behavior under static loading initially was realized through back-analysis of foundation and excavation movements in the United Kingdom (Burland, 1989). The recognition of zones of high initial stiffness under typical field conditions was followed by efforts to measure this ubiquitous behavior in the laboratory for various types of soil (Jardine et al, 1984; Clayton and Heymann 2001; Santagata et al. 2005; Callisto and Calebresi 1998, Holman 2005, Cho 2007). Furthermore, the stiffness depends on the direction of loading, as measured from the most recently applied stress path, or recent stress history.

To illustrate small strain nonlinearity and recent stress history effects on shear stiffness for Chicago clays, secant shear modulus from drained constant mean normal stress (CMS) and constant mean normal stress extension (CMSE) stress paths are plotted versus shear strains in Figure 3. These specimens with an OCR of 1.7 were obtained from block samples cut from an excavation in Evanston, IL (Blackburn and Finno 2007). In all cases, the secant shear modulus at 0.1% strain, the smallest strain reliably measured in conventional triaxial equipment, was about 4 times less than that measured at 0.002% strain, the smallest value obtained with the internal instrumentation used in these experiments (Cho 2007).

In Figure 3, the angles noted next to the stress paths are calculated as an angle change from the previous stress path ($\theta = 0°$) without consideration of rotation direction. The results of the two "K_0" probe tests showed dependence on the angle change, with the CMSE path (unloading) exhibiting a stiffer response than that of the CME (loading type). For the "post-unloading" probe tests, with a recent stress history representative of a site where an old building with a basement was demolished before excavation, the opposite directional dependency is observed. The stiffness of loading path (U-CMS) is much greater than those of unloading path (U-CMSE). Interestingly, shear moduli magnitudes in the loading path (K_0-CMS) of the "K_0" probes and the unloading path (U-CMSE) of the "post-unloading" probes with similar values of θ are quite alike, even though the current stress path direction is exactly the opposite. Considering the change in θ, as shown in the inset of Figure 3, the stiffer shear moduli occur at the stress path corresponding to nearly complete stress reversals, U-CMS (θ =160°) and K_0-CMSE (θ =147°). Although the data are limited, it shows the effects of recent stress history on the shear stiffness. Also, little difference was noted at strains larger than 0.1%, as reported by Atkinson et al (1990). Thus is appears that recent stress history effects are significant for these clays – G_{sec} at about 0.002% strain varies by a factor of 2. Complete details and results of the testing program are presented by Cho (2007).

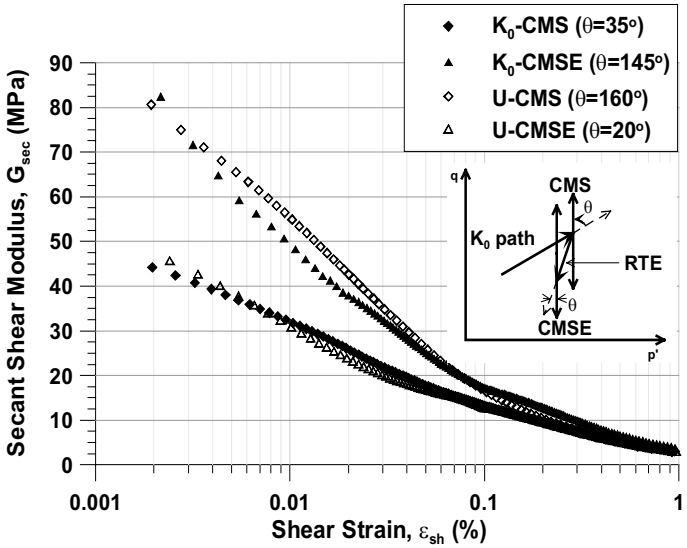

Figure 3. Recent stress history effects on secant shear modulus: Chicago glacial clay

Burland (1989) suggested that working strain levels in soil around well-designed tunnels and foundations were on the order of 0.1 %. If one uses data collected with conventional triaxial equipment to discern the soil responses, in many practical situations, it is not possible to accurately incorporate site-specific small strain non-linearity into a constitutive model based on conventionally-derived laboratory data.

There are a number of models reported in literature wherein the variation of small strain nonlinearity can be represented, for example, a three-surface kinematic model develop for stiff London clay (Stallebrass and Taylor 1997), MIT-E3 (Whittle and Kavvadas 1994), hypoplasticity models (e.g. Viggiani and Tamagnini 1999), and a directional stiffness model (Tu 2007). These models require either detailed experimental results or experience with the model in a given geology to derive parameters. Alternatively, one can use a neural network based constitutive model wherein the constitutive response is learned based on observed field and laboratory data. More work is needed to relate these actual soil responses to conventionally-obtained field and laboratory data in order to incorporate these responses into practice.

For most current practical applications, one uses simpler, elasto-plastic models contained in material libraries in commercial codes. For these models, a key decision is to select the elastic parameters that are representative of the secant values that correspond to the predominant strain levels in the soil mass. Examples of the strain levels behind

a wall for an excavation with lateral wall movements of 29 and, 57 mm are shown in Figure 4. These strain levels were computed based on the results of displacement-controlled simulations where the lateral wall movements and surface settlements were incrementally applied to the boundaries of a finite element mesh. The patterns of movements were typical of excavations through clays, and were based on those observed at an excavation made through Chicago clays (Finno and Blackburn 2005). Because the simulations were displacement-controlled, the computed strains do not depend on the assumed constitutive behavior.

As can be seen in Figure 4, the maximum shear strains correspond to about 0.3% for 29 mm maximum wall lateral movement, and represent good control of ground movements in these soft soils. Shear strains as high as 0.7% occurred when 57 mm of maximum wall movement develop. These strain levels can be accurately measured in conventional triaxial testing, and thus if one can obtain specimens of sufficiently high quality, then secant moduli corresponding to these strain levels can be determined via conventional laboratory testing. Because the maximum horizontal wall displacement can be thought of as a summation of the horizontal strains behind a wall, the maximum wall movements can be accurately calculated with a selection of elastic parameters that correspond to these expected strain levels. In Figure 4, the fact that small strain non-linearity is not explicitly considered will not have a large impact on the computed horizontal wall displacements because they are dominated by the larger strains in the soil mass. Consequently, these computed movements would be compatible with those measured by an inclinometer located close to the wall.

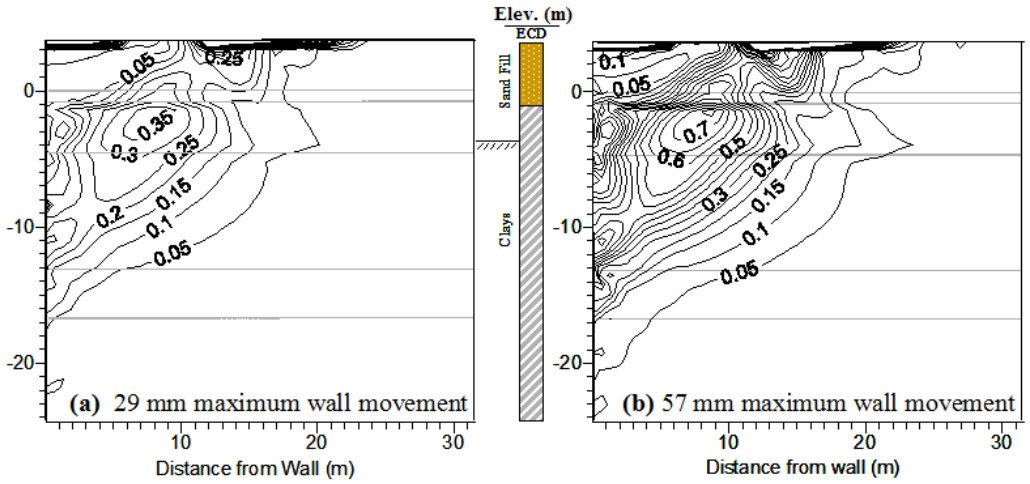

Figure 4. Shear strain levels behind excavation (contours in %)

However, if one needs to have an accurate representation of the distribution of ground movements with distance from the wall, then this approach of selecting strain-level appropriate elastic parameters will not work. The small strain non-linearity must be explicitly considered to find the extent of the settlement because the strains in the area of interest vary from the maximum value to zero. As a consequence, many cases reported in literature indicate computed wall movements agree reasonably well with observed values, but the results from the same computations do not accurately reflect the distribution of settlements. Good agreement at distances away from a wall can be obtained only if the small stain non-linearity of the soil is adequately represented in the constitutive model.

3. Monitoring Data

The assumptions inherent in any prediction limit the types of data that can be used as a basis of updating performance predictions. Consequently, one must carefully select the types of data, location of the measuring points, and the excavation conditions when applying an inverse technique. Inclinometer data based on measurements close to a support wall are the most useful when typical elasto-plastic constitutive models are assumed to represent soil

behavior, as is the case when employing commercial finite element codes, for reasons discussed in the last section. These data can be supplemented by ground surface settlements when using a constitutive model that accounts for small strain nonlinearities and dilation (Finno and Tu 2006, Hashash and Whittle, 1996). Furthermore, other types of measurements, such as forces in internal braces and pore water pressures, conceptually can be used in conjunction with displacement measurements to make the computed results more sensitive to parameters selected for optimization (Rechea 2006).

While these different types of data can be handled within a properly formulated inverse analysis, the timely collection and screening of the data must be successfully accomplished. Furthermore, for any monitoring system to be fully automated, one must be able to track construction progress so that performance data can be correlated with the excavation activities. To correlate the numerical data with the causative actions of the excavation process, imaging technologies can be employed to provide an accurate and detailed record of construction activities. Trupp et al. (2004) and Su et a. (2006) used 3-D laser scanning to capture an accurate image of the geometry of the excavation to provide an accurate, as-built digital record of construction. Sections may be taken from these scans and imported into a finite element code to provide an accurate excavation surface for input to inverse analysis. An internet accessible weather-resistant video camera has been used on several projects to allow remote visualization of the construction process in real-time, as well as a dated, photographic record of construction (Finno and Blackburn 2005). Significant developments have been made in automated systems to continuously monitor deformations due to construction activities. These systems provide the engineer with uninterrupted stream of data in near real time without the need to wait for manual data readings. Such systems are essential tools for making timely decisions regarding changes in construction activities and support installation to mitigate potential damage to adjacent facilities. A number of these and examples of their use are included in the following sections.

3.1 Laser Scanning

Three-dimensional laser scanning is a relatively new technology that utilizes LIDAR (Light Detection and Ranging). It is similar to RADAR (Radio Detection and Ranging), but uses light to measure range or distance. A laser scanner consists of an emitting diode that produces a light source at a very specific frequency. A mirror directs the laser beam (with a diameter of 6 mm) horizontally and vertically towards the target. The surface of the target then reflects the laser beam. Using the principles of pulse time of flight the distance can be determined by the transit time, with a precision of +/- 6 mm. The result of a scan produces point clouds and is processed into accurate 3D models, as illustrated in Figure 5.

Figure 5. Photo and scanned terrain mesh for Ford Center Excavation

One must acquire accurate records of construction staging in deep excavations to understand and predict the field responses to excavation as well as impacts on nearby facilities. The practical use of laser scanning for this purpose was demonstrated at the Ford Center excavation in Evanston, Il (Trupp et. al. 2004). With dimensions of 36 m x 45 m (length x width), an excavation supported by an internally-braced sheet pile wall was made between mid-January and mid-May, 2004. During this entire period a laser scanner was employed weekly to carry out the 3-D field scanning. The scans provide 3-D to scale geometric dimensions of the excavation, as illustrated in Figure 5. In the scanned image, the internal bracing and backhoe were removed for clarity. The terrain model can be automatically imported into a numerical simulation environment to improve the fidelity of model simulation. This information can be used for construction management functions as well and to develop as-built drawings of unprecedented accuracy.

3.2 Webcams

Internet accessible weather-resistant video cameras ("webcam") can be employed at a project to track and record construction activities in real-time. The camera shown on Figure 6 was used to track the construction progress at the Olive 8 excavation in Seattle. Webcams can be installed with features that allow a password restricted user to pan and zoom to allow details of the construction to be observed. The images can be made accessible via a website to the general public, including project engineers, contractors and owners. The images also can be combined with the automated survey and tiltmeter data to observe the response to the excavation process in real-time from a remote location and to relate it qualitatively to construction operations. Laser scan images can be used to relate such data quantitatively, as described by Quiñones-Rozo et al. (2008).

a) Total station and webcam b) Communications link

Figure 6. Total Station and webcam at Olive 8 excavation

3.2 Automated Total Surveying Station

Robotic total surveying stations can be used to monitor the displacement of optical prisms placed at various locations around an excavation site**.** Use of such a system at the Olive 8 excavation in Seattle, WA, illustrates its capabilities (Finno and et al. 2007). This project involved construction of a 39 story structure with 5 levels of below grade parking. The 76 ft deep excavation next to an adjacent building required a hybrid support system consisting of large soldier piles with tightly spaced soil nails in the upper portion and steeply inclined tieback anchors in the lower portion (Figure 7). The total station shown in Figure 6 was accessible via the Internet. A commercial 802.11 wireless-to-Ethernet network bridge and VPN router inside the communication box provided the connection. A

point-to-point radio link was established between the enclosure and a telephone modem in the nearby construction field office. This data link provided a backup communication method when the wireless Internet service was disrupted. Custom software on an embedded Linux computer inside the enclosure recorded data from the total station. It also recorded photos to provide a visual record of the construction activities during excavation. A custom-built, digitally-controlled power switch enabled the embedded computer to cycle power to the total station when its internal computer lost power.

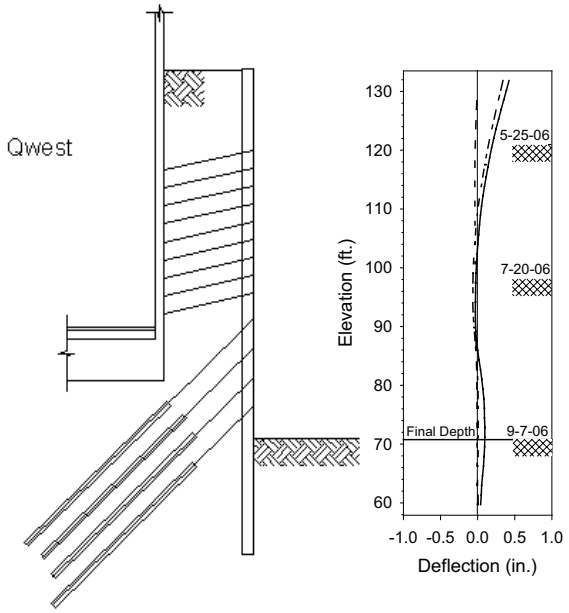

Figure 7. Lateral movements measured behind wall

All point position data are calculated relative to at least two fixed reference points which allows for slight instrument movement during operation and allows the instrument to be removed for repairs, if necessary. Also, by calculating the positions of the reference points relative to each other, instrument tilt can be detected. Accuracy of the system was computed to be ± 2.8 mm.

Figure 7 summarizes the lateral movements behind the wall during excavation. Similar responses were observed at other sections. A cantilever movement profile was observed as the soil was excavated to elev. 97.1 ft. The maximum movement at the top of the soldier pile wall was 0.42 inches. The reinforcing effect of soil nails is clearly seen in that little lateral deflection recorded at the level of the soil nails. As the excavation was made to elevation +71.5 ft., small lateral movements were observed on the order of 0.1 inch. Most of the cantilever movement was obtained by the time that the excavation level reached +97.1 ft, or about ½ the full depth of the case. Thereafter small deep seated movements developed.

Lateral movements both perpendicular and parallel to the excavation at the top of the wall at the same location are plotted versus time in Figure 8. It can be seen that the data collected by the total station and inclinometer agree quite well throughout the entire excavation. The movements parallel to the excavation measured by both the inclinometer and total station were negligible at this instrument section.

The data collected during the excavation showed that the as-constructed hybrid support system was stiff enough such that lateral movements were less than the 1 inch limitation imposed by the City of Seattle. In fact, the maximum observed movement was about one-half of the limit. The web-based display of the data and the combination of the more frequent total station data and the inclinometer data allowed the engineers, contractor and the City to assess the performance of the wall during construction, and, because of the better than expected performance, additional lateral support was not needed. This approach worked particularly well for this case because the maximum movements were expected to be the lateral movements at the top of the support walls, and the

automated system was capable of measuring this key data. This information would not have been as useful as an indicator of performance if the maximum movements occurred at or near excavated grade, as is common for many supported excavations.

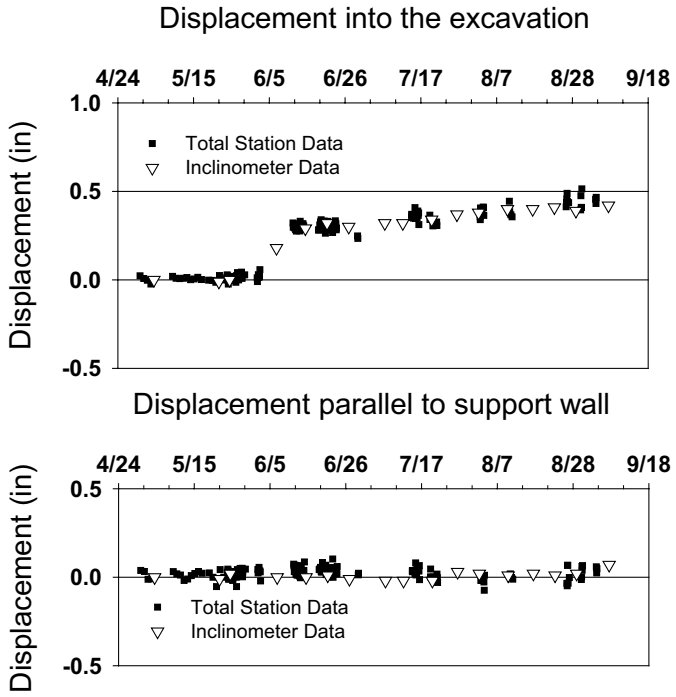

Figure 8. Comparison between Inclinometer and Total Station Data

3.3 Remote Access Tiltmeters

Tilt is important because it allows one to compute the angular distortion – a parameter that is correlated with observed damage – if the settlement distribution is known. Correlating tilt measurements to ground movements allows the structural response of an affected building to the excavation activities to be directly evaluated when coupled with structural models (e.g. Finno et al. 2005). After all, it is protection of the adjacent structures that is the design objection in many excavations in congested urban areas.

Remote access tiltmeters can be mounted on selected structural elements of the building affected by excavation activities to monitor the response of the structure during excavation. To illustrate the use of these instruments, remote access tiltmeter pairs were installed on support members in the basement of the Tech building adjacent to the Ford Center excavation. They were attached to the structure with a quick-setting epoxy and coupled with Freewave point-to-point radio transceivers to allow continuous remote data collection (Blackburn et al. 2005). The Tech Building spread footings are placed atop clay strata in which the strength increases with depth, except for a crust at the top of the sequence. If the deformation in the underlying clay layers is assumed to be undrained (with zero volume change), then the vertical settlement distribution at the footing elevation can be approximated by rotating the lateral movements from an inclinometer about a pivot point at a depth corresponding to the inclinometer distance from the wall (Finno, et al. 2002), as illustrated in Figure 9a. The slope of the footing at each column location is estimated from the rotation of the slope inclinometer deformation pattern. Tiltmeters installed on support columns just above the floor slab of Tech recorded the column tilt as the footing deforms with the soil. When the tiltmeter results are compared with the expected slope at each footing location, the difference between the two is caused by restraint from the superstructure and the stiffness of the column-footing connection. For a rigid connection, the tilt equals the slope.

Figure 9b shows measured tilt values at the wall and second column in the north/south direction, the slope of the footing from inclinometer 1 data, the distortion between the wall and first interior column, and a brief construction record. The distortion is the relative settlement between the wall and the second column divided by the distance between the two and depends on the structural stiffness of the building. Initially, the clay soil heaves away from the excavation as a result of installing the sheeting around day 50, resulting in heave of the structure. This movement is more pronounced in the clay, so the maximum heave occurs at some distance from the south end of the building, resulting in more heave at the column. The distortion to the south, implying that the column heaved more than the wall, reflects this response, as does the tilt of both column and wall. As the excavation progresses and the soil moves toward the excavation, both the column and wall footing settle. The wall tilts towards the north at approximately the same rate as the soil slope from the inclinometer data, suggesting an almost rigid connection between the thick masonry wall and underlying strip footing. The magnitude of the tilt observed at his location approached a slope of 0.0015, or 1/667. Tilt of the second column does not mimic the slope of the inclinometer data at the corresponding depth between days 62 and 140, but rather more closely mimicked the distortion. This pattern of movement suggests a more flexible connection between the footing and the column, as one would expect for an isolated column on a spread footing as compared to a thick wall on a strip footing. After day 140 when the excavation had reached its final depth, the column tilt of less than 1/2000 was approximately equal to the slope of the footing. Despite these levels of column tilting and footing deformations, no structural or cosmetic damage to the Tech Building was detected in this direction during the excavation.

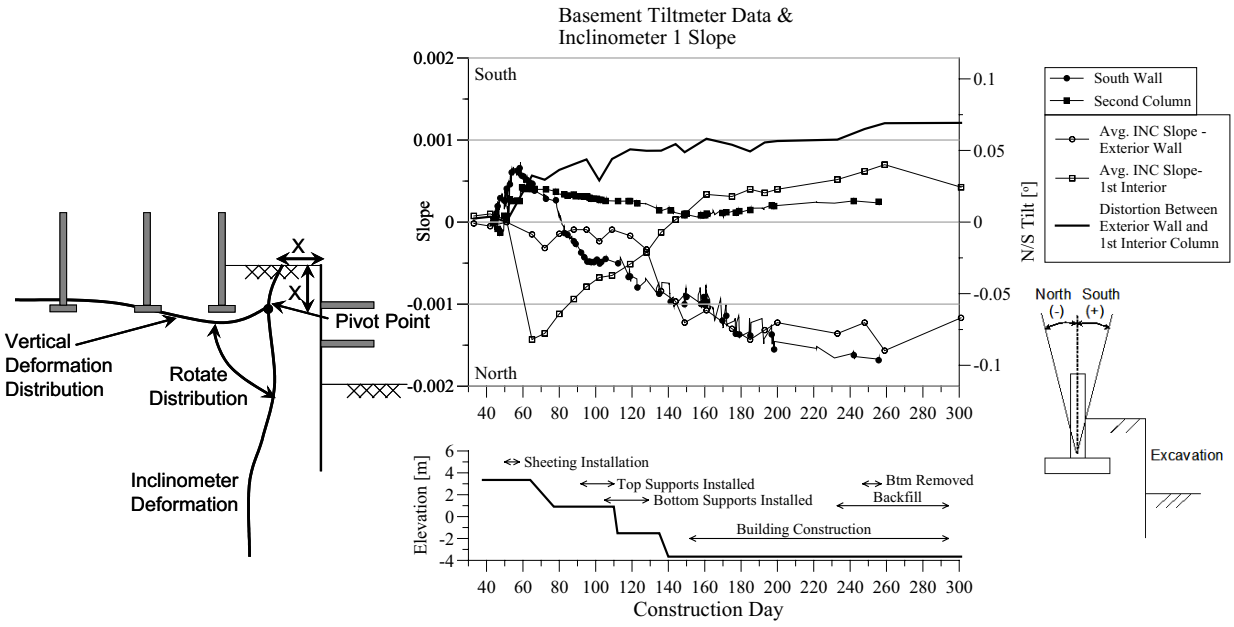

a) Soil settlement profile from inclinometer data

b) Tilt of structure at several locations

Figure 9. Tilt meter installation and observed responses at the Ford Center excavation

3.4 In-place Inclinometers

Inclinometers placed close behind a support wall are a particularly good source of observations against which state-of-the-practice predictions can be evaluated and updated using inverse procedures described later. However, data collection is tedious and many times the data is not transmitted to interested parties in a timely fashion. To apply these measurements in an automated system, use of in-place inclinometers would be quite useful. However, proven

systems are quite expensive when the proper number of measuring points is installed at a given location. Recently-developed MEMS-based in-place inclinometer systems provide a low-cost alternative.

Data from an in-place inclinometer is plotted on Figure 7. The sensors in this system are based on MEMS technology, and an automated system was used to collect and display the data on a password-protected website. These data were collected over a 4 month period at an excavation site prior to any construction activity at the inclinometer location, so one would expect no movements to occur during this period. Both temperature and lateral movement measurements were not accurate after about 1.5 months of service. Results from a conventional inclinometer placed within several meters of the automated system verified that no lateral movement occurred. Upon inquiry, the manufacturer of the sensor (not of the inclinometer) stated that the particular sensor used in the system drifts and should not be used for long-term applications. This is a particularly bad feature for a system with as many as 2 sensors for every 2 ft of inclinometer, all of which can drift at different rates. While one should not condemn all MEMS sensors for use in excavation applications, it is prudent to check with the *sensor* developer regarding stability of the actual sensor in a system.

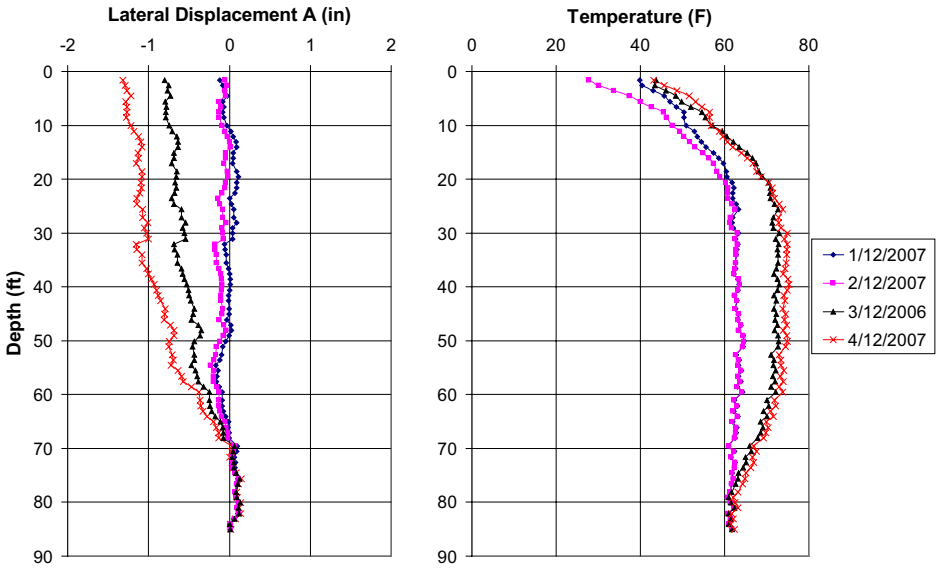

Figure 10. Drift in MEMS-based inclinometer

4. Self-updating Models

Self-updating models can be of two types, one wherein the constitutive responses are assumed and key parameters of the model are updated using inverse techniques based on selected field observations, and the other wherein the field observations are used to define the constitutive response using artificial neural nets.

Inverse analysis techniques have been applied to geotechnical problems since the 1980s (e.g., Gioda and Maier 1980; Sakurai and Takeuchi 1983). Its use allows one to evaluate performance of geotechnical structures by a quantifiable observational method. It has been used to identify soil parameters from laboratory or in situ tests (e.g., Anandarajah and Agarwal 1991), and performance data from excavation support systems (e.g., Ou and Tang1994; Calvello and Finno 2004; Finno and Calvello 2005; Levasseur et al. 2007), excavation of tunnels in rock (Sakurai and Takeuchi, 1983; Gens et al. 1996) and embankment construction on soft soils (Arai et al., 1986; Wakita and Matsuo, 1994). Many of the previous evaluations of performance data were conducted with very simple soil models

that severely restricted the ability of the computations to accurately reflect the observed field performance data, irrespective of employing inverse techniques.

Use of an inverse model provides results and statistics that offer numerous advantages in model analysis and, in many instances, expedites the process of adjusting parameter values. The fundamental benefit of inverse modeling is its ability to calculate automatically parameter values that produce the best fit between observed and computed results. The main difficulties inherent to inverse modeling algorithms are complexity, non-uniqueness, and instability. Complexity of real, non-linear systems sometimes leads to problems of insensitivity when the observations do not contain enough information to support estimation of the parameters. Non-uniqueness may result when different combinations of parameter values match the observations equally well. Instability can occur when slight changes in model variables radically change inverse model results. Although these potential difficulties make inverse models imperfect tools, work in related civil engineering fields (e.g., Poeter and Hill, 1997) demonstrate that inverse modeling provides capabilities that help modelers significantly, even when the simulated systems are very complex.

Two main types of inverse analysis have been applied to excavatons, optimization by iterative algorithms such as gradient methods (e.g., Ou and Tang 1994; Ledesma et al., 1996; Calvello and Finno 2004) and optimization by techniques from the field of artificial intelligence, including artificial neural networks (Yamagami et al. 1997; Hashash et al. 2006) and genetic algorithms (Levasseur et al. 2007). The gradient method employs a local parameter identification of a specific constitutive law. The artificial neural network is a method which creates by learning phases its own constitutive law from geotechnical measurements. Genetic algorithms are global optimization methods which localize an optimum set of solutions close to the "true" value. This paper will discuss a gradient method approach.

4.1 Gradient Method

The gradient method described herein uses UCODE (Poeter and Hill, 1998), a computer code designed to allow inverse modeling posed as a parameter estimation problem. Macros can be written in a windows environment to couple UCODE with any application software.

Figure 11 shows a flowchart of the parameter optimization algorithm used in UCODE. With the results of a finite element prediction in hand, the computed results are compared with field observations in terms of weighted least-squares objective function, S(b):

$$S(\underline{b}) = \left[\underline{y} - \underline{y}'(\underline{b})\right]^T \underline{\omega}\left[\underline{y} - \underline{y}'(\underline{b})\right] = \underline{e}^T \underline{\omega e} \tag{1}$$

where $\underline{b}$ is a vector containing values of the parameters to be estimated; $\underline{y}$ is the vector of the observations being matched by the regression; $\underline{y'(b)}$ is the vector of the computed values which correspond to observations; $\underline{\omega}$ is the weight matrix wherein the weight of every observation is taken as the inverse of its error variance; and $\underline{e}$ is the vector of residuals. This function represents a quantitative measure of the accuracy of the predictions.

A sensitivity matrix, $\underline{X}$, is then computed using a forward difference approximation based on the changes in the computed solution due to slight perturbations of the estimated parameter values. This step requires multiple runs of the finite element code. Regression analysis of this non-linear problem is used to find the values of the parameters that result in a best fit between the computed and observed values. In UCODE, this fitting is accomplished with the modified Gauss-Newton method, the results of which allow the parameters to be updated using:

$$\left(\underline{C}^T \underline{X}_r^T \omega \underline{X}_r \underline{C} + \underline{I}\, m_r\right)\underline{C}^{-1}\underline{d}_r = \underline{C}^T \underline{X}_r^T \omega\left(\underline{y} - \underline{y}'(\underline{b}_r)\right) \tag{2}$$

$$\underline{b}_{r+1} = \rho_r \underline{d}_r + \underline{b}_r \tag{3}$$

where d_r is the vector used to update the parameter estimates b; r is the parameter estimation iteration number; X_r is the sensitivity matrix ($X_{ij}=\partial y_i/\partial b_j$) evaluated at parameter estimate $\underline{b}_r$; $\underline{C}$ is a diagonal scaling matrix with elements c_{jj}

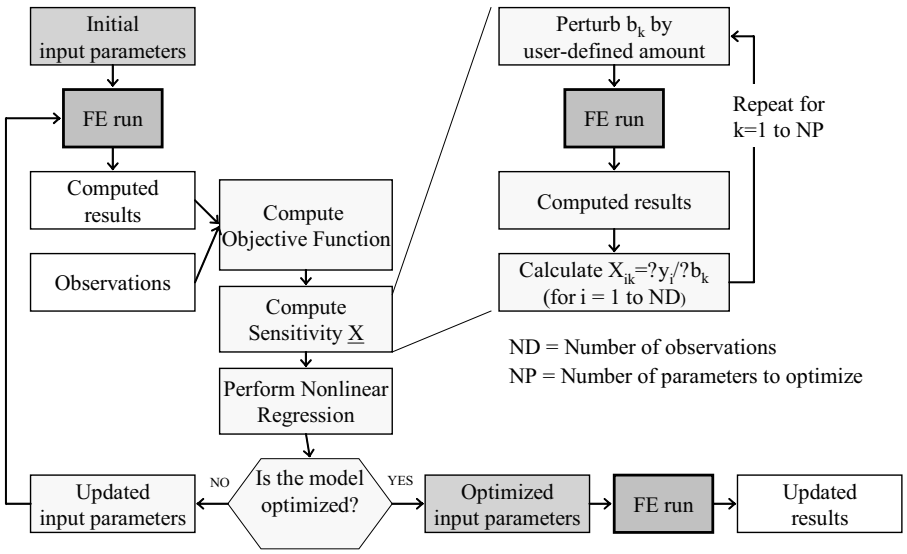

Figure 11. Flow chart for gradient method

equal to $1/\sqrt{(\underline{X}^T \underline{\omega}\ \underline{X})_{jj}}$; $\underline{I}$ is the identity matrix; m_r is the Marquardt parameter used to improve regression performance; and $\underline{d}_r$ is a damping parameter, computed as the change in consecutive estimates of a parameter normalized by its initial value, but is restricted to values less than 0.5.

At a given iteration, after performing the modified Gauss-Newton optimization, the updated model is considered optimized if either of two convergence criteria is met: (i) the maximum parameter change of a given iteration is less than a user-defined percentage of the value of the parameter at the previous iteration; (ii) the objective function, $S(\underline{b})$, changes less than a user-defined amount for three consecutive iterations.

After the model is optimized, the final set of input parameters is used to run the finite element model one last time and produce the "updated" prediction of future performance. See Rechea (2006) for details concerning the convergence criteria as applied to excavations.

4.2 Weighting Function

The weight of an observation can be expressed as the inverse of the variance for the 95% confidence interval for the accuracy of a measurement:

$$weight = \frac{1}{\sigma^2} \qquad \sigma = \frac{Accuracy}{1.96} \tag{4}$$

In this way, more reliable data (smaller variability) are given greater emphasis, or weight. The errors associated to measurements are usually related to the accuracy of the instrumentation, and independent of the magnitude of the observation (assuming the observation is within the range of the instrumentation). Table 1 shows how to obtain weights for various types of instrumentation. Accuracies and ranges in Table 1 are taken from manufacturer's literature, and are meant to be representative of typical values in the field. Smaller values can be used based on field data collected prior to any activity at the site, assuming enough data are collected to adequately define the variation about the initial value (Langousis 2007).

Table 1: Typical weights of observations

Instrumentation	Range (full scale)	Accuracy	95% standard deviation, σ	Weight
Lateral movements with inclinometers	± 53° from vertical	± 0.25 mm/m $\frac{0.25}{1000}\cdot d$	$\frac{0.25}{1000}\cdot\frac{d}{1.96}=0.0001\cdot d$ (m)	$\frac{1}{(0.0001\cdot d)^2}$
		where d is distance (m) from bottom of casing		
Ground surface settlement with optical survey		± 0.01 ft ± 0.003 m	$\frac{0.003}{1.96}=0.00155$ (m)	$\frac{1}{(0.00155)^2}$
vibrating wire piezometer	3.5 bar/50 psi 344.8 Pa	± 0.1% FS ± 0.34 Pa	$\frac{0.34}{1.96}=0.173$ (Pa)	$\frac{1}{(0.173)^2}$
Strut force with spot-weldable strain gauge	2,500 microstrain	± 0.1%FS = ± 2.5 microstrain	$\frac{E\cdot A\cdot Accuracy}{1.96}$ (kN)	$\frac{1}{(6.19)^2}$ (1)

(1) value shown is for a steel brace with A = 0.024 m^2

4.3 Selection of Parameters

The relative importance of the input parameters being simultaneously estimated can be defined using various parameter statistics (Hill 1998). The statistics found useful for this type of work are the composite scaled sensitivity, ccs_j, and the correlation coefficient, *cor(i,j)*. The value of css_j indicates the total amount of information provided by the observations for the estimation of parameter j, and is defined as:

$$css_j = \left[\sum_{j=1}^{ND}\left(\left(\frac{\partial y'_i}{\partial b_j}\right)b_j\omega_{ii}^{1/2}\right)^2\Bigg|_{\underline{b}}\Big/ND\right]^{1/2} \tag{5}$$

where y'_i is the i^{th} computed value, b_j is the j^{th} estimated parameter, $\partial y_i/\partial b_j$ is the sensitivity of the i^{th} computed value with respect to the j^{th} parameter, ω_{ij} is the weight of the i^{th} observation, and ND is the number of observations.

The values of the matrix *cor (i,j)* indicate the correlation between the i^{th} and j^{th} parameters, and are defined as:

$$cor(i,j)=\frac{\mathrm{cov}(i,j)}{\mathrm{var}(i)^{1/2}\,\mathrm{var}(j)^{1/2}} \tag{6}$$

where cov(*i,j*) equal the off-diagonal elements of the variance-covariance matrix $\underline{V}(\underline{b}')=s^2(\underline{X}^T\underline{\omega}\underline{X})^{-1}$, and var(*i*) and var(*j*) refer to the diagonal elements of $\underline{V}(\underline{b}')$.

Inverse analysis algorithms allow the simultaneous calibration of multiple input parameters. However, identifying the important parameters to include in the inverse analysis can be problematic, and it is not possible to use a regression analysis to estimate every input parameter of a given excavation simulation. The number and type of input parameters that one can expect to estimate simultaneously depend on a number of factors, including the soil models used, the stress conditions of the simulated system, available observations, and numerical implementation issues. Examples of this procedure are presented by Calvello and Finno (2004) and Finno and Calvello (2005).

5. Capabilities of Adaptive Management Method

Several examples of the gradient method applied to supported excavations are presented to illustrate (i) its ability to identify optimized parameters based on observations made during early stages of excavation so as to allow accurate

predictions of performance of latter stages of an excavation, and, (ii) the applicability of optimized parameters found based on performance data of one excavation to others in the same geology.

The finite element software PLAXIS was used to compute the plane strain response of the soil around these excavations. The inverse techniques contained in UCODE can be coupled with any application software, and it also has been successfully coupled with ABAQUS and other research-oriented finite element codes. For purposes of brevity, only PLAXIS applications with the hardening-soil model (H-S) (Schanz et al. 1999) are presented in this paper. Parameters from other constitutive models have been optimized as well (e.g., Calvello and Finno 2002).

The effective stress H-S model is formulated within the framework of elasto-plasticity. Plastic strains are calculated assuming multi-surface yield criteria. Isotropic hardening is assumed for both shear and volumetric strains. The flow rule is non-associative for frictional shear hardening and associative for the volumetric cap. Six basic H-S input parameters define the constitutive soil responses, the friction angle, φ, cohesion, c, dilation angle, ψ, the reference secant Young's modulus at the 50% stress level, E_{50}^{ref}, the reference oedometer tangent modulus, E_{oed}^{ref}, and the exponent *m* which relates reference moduli to the stress level dependent moduli (E representing E_{50}, E_{oed}, and E_{ur}):

$$E = E^{ref}\left(\frac{c\cot\phi - \sigma_3^{'}}{c\cot\phi + p^{ref}}\right)^{m} \tag{7}$$

where p^{ref} is a reference pressure equal to 100 stress units and σ'_3 is the minor principal effective stress. A sensitivity analysis indicated that the model's relevant and uncorrelated parameters for the Chicago excavations presented herein are E_{50}^{ref} and φ' (Calvello and Finno 2004). Results were also sensitive to changes in values of parameter *m*. However, parameter *m* was not included in the regression because the values of the correlation coefficients between parameters *m* and E_{50}^{ref} were very close to 1.0 at every layer, indicating that the two parameters were not likely to be simultaneously and uniquely optimized. When values of φ' were kept constant at their initial estimates, and only the stiffness parameters, E_{50}^{ref}, were optimized, the calibration of the simulations presented subsequently was successful. Finno and Calvello (2005) showed that shear stress levels in the soil around the excavation were much less than those corresponding to failure for the great majority of the soil. This is indeed expected for excavation support systems that are designed to restrict adjacent ground movements to acceptably small levels, and hence one would expect the stiffness parameters to have a greater effect on the simulated results than failure parameters.

5.1 Parameter Optimization at Early Stages of Excavation

The ability of the approach to provide optimized parameters at an early stage of excavation which leads to good predictions of subsequent performance is illustrated by the Chicago Ave. and State St. subway renovation project in Chicago (Finno et al. 2002). This project involved the excavation of 12.2 m of soft to medium clay within 2 m of a school supported on shallow foundations. Figure 12 shows a section of the excavation support system and the subsurface conditions. The support system consisted of a secant pile wall with three levels of support, which included pipe struts (1st level) and tieback anchors (2nd and 3rd levels). The subsurface conditions consisted of an urban fill, mostly medium dense sand but also containing construction debris, overlying four strata associated with the repetitive process of advance and retreat of the Wisconsin glacier. The upper three are ice margin deposits deposited underwater, and are distinguished by water content and undrained shear strength (Chung and Finno, 1992). With the exception of a clay crust in the upper layer, these deposits are lightly overconsolidated as a result of lowered groundwater levels after deposition and/or aging. Stratigraphy is shown in terms of Chicago City Datum (CCD) elevation.

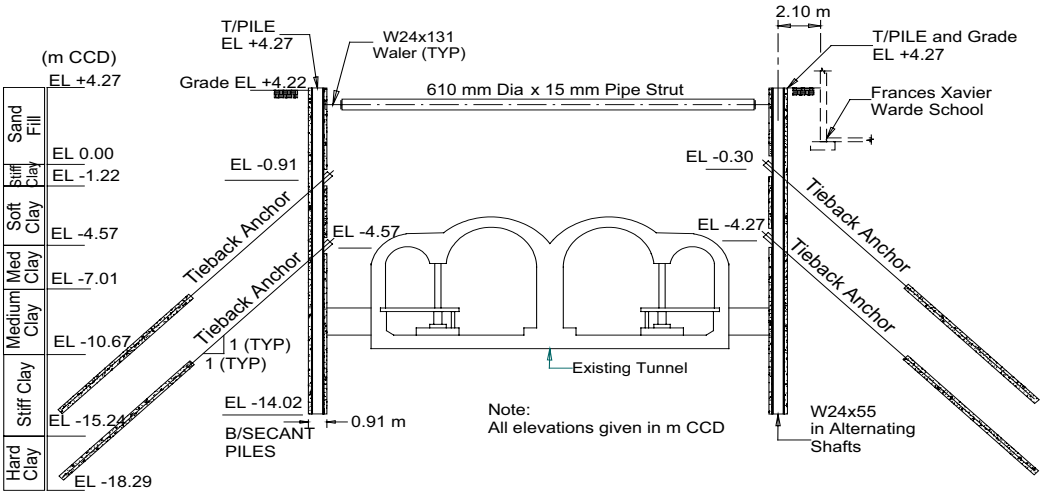

Figure 12. Support system for Chicago-State excavation (Finno et al. 2002)

A complete record of performance of the excavation can be found in Finno et al. (2005). Figure 13 summarizes deformation responses to excavation and support. Both lateral movements and settlements are shown. The movements that occurred as the secant pile wall extend through all compressible layers. This is important when using these observations to calibrate parameters using inverse techniques in that these movements occur at an early stage of the excavation, and hence contain information that can be used to optimize parameters in all layers that can be useful to predict movements at subsequent stages of excavation. It is important to realize that the H-S model used for this analysis did not include effects of small strain non-linearity and hence relatively large movements were needed before any adjustments could be made to the model parameters and the surface settlements could not be used to optimize the parameters.

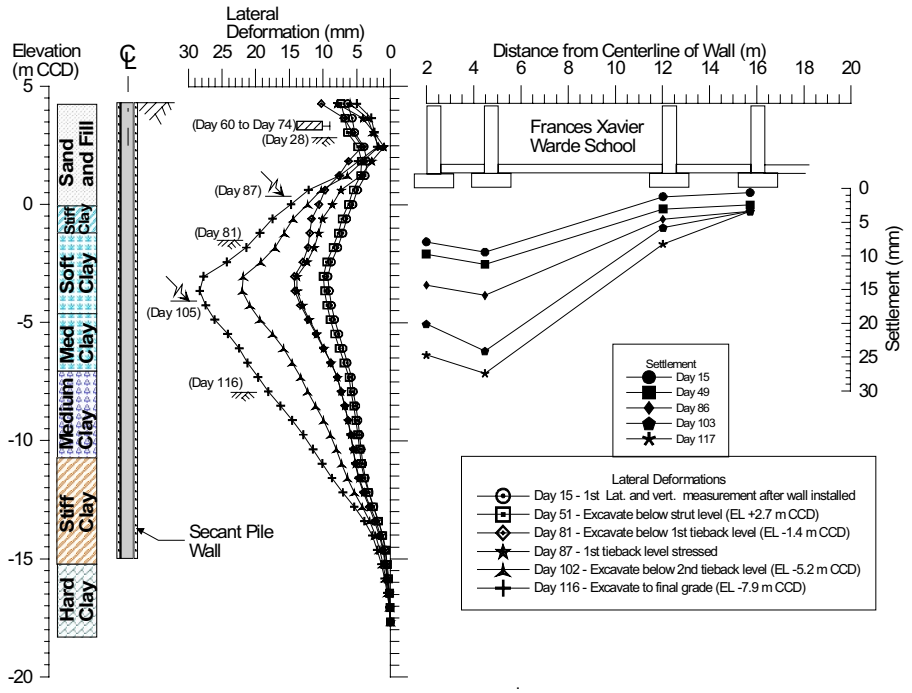

Figure 13. Lateral movements and settlements at Chicago-State excavation (Finno et al. 2002)

Very little movement beyond that which occurred during wall installation were observed until the excavation was lowered below EL. –1.4 m CCD; a maximum of 4 mm additional lateral movement occurred as a result of excavating to this elevation. This behavior suggests that the upper clays initially are relatively stiff, and provide field indications of the small strain nonlinearity of these soils. After wall installation, the secant pile wall incrementally moved toward the excavation in response to excavation-induced stress relief. When the excavation reached final grade, the maximum lateral movement was 28 mm. The school settled as the secant pile wall moved laterally. The maximum settlement at the school at the end of excavation was also 28 mm.

Table 2 shows the calculation phases and the construction stages used in the finite element simulations. Note that the tunnel tubes and the school adjacent to the excavation were explicitly modeled in the first 12 phases of the simulation to take into account the effect of their construction on the soil surrounding the excavation. Stages 1, 2, 3, 4 and 5 in the optimization process refer to the construction stages for which the computed results were compared to inclinometer data taken from two inclinometers on opposite sides of the excavation. Construction steps not noted as "consolidation" on Table 2 were modeled as undrained. Consolidation stages were included after the tunnel, school and wall installation calculation phases to permit excess pore water pressures to equilibrate. To simulate secant pile wall installation in the plane strain analysis, elements representing the wall were excavated and a hydrostatic pressure equivalent to a water level located at the ground surface was applied to the face of the resulting trench (calculation phase 13 in Table 2). After computing the movements associated with this process, the excavated elements were replaced by elements with the properties of the secant pile wall (calculation phase 14). Details about the definition of the finite element problem, the calculation phases and the model parameters used in the simulation can be found in Calvello (2002).

Visual examination of the horizontal displacement distributions at the inclinometer locations provides the simplest way to evaluate the fit between computed and measured field response. When computations were made based on parameters derived from results of drained triaxial tests, the finite element model computed significantly larger displacements at every construction stage (Finno and Calvello 2005). The maximum computed horizontal displacements are about two times the measured ones and the computed displacement profiles result in significant and unrealistic movements in the lower clay layers. As one would expect, these results indicated that the stiffness properties for the clay layers based on conventional laboratory data were less than field values.

Table 2. FE simulation of construction

Phase	Construction step	Simulation stage
0	Initial conditions	
1-4 5	Tunnel construction (1940) Consolidation	
6-10 11-12	School construction (1960) Consolidation	
13	Drill secant pile wall (1999)	
14	Place concrete in wall	Stage 1
15	Consolidation (20 days)	
16	Excavate and install struts	Stage 2
17	Excavate below first tieback level	
18	Prestress first level of tiebacks	Stage 3
19	Excavate below second tieback level	
20	Prestress second level of tiebacks	Stage 4
21	Excavate to final grade	Stage 5

Figure 14 shows the comparison between the measured field data from both sides of the excavation and the computed horizontal displacements when parameters are optimized based on stage 1 observations. The improvement of the fit between the computed and measured response is significant. Despite the fact that the optimized set of parameters is calculated using only stage 1 observations, the positive influence on the calculated response is substantial for all construction stages. At the end of the construction (i.e. stage 5) the maximum computed displacement exceeds the

measured data by only about 15%. These results are significant in that a successful recalibration of the model at an early construction stage positively affects subsequent "predictions" of the soil behavior throughout construction.

Analyses were also made wherein parameters were recalibrated at every stage until the final construction stage (stage 5). At every new construction stage, the inclinometer data relative to that stage were added to the observations already available. Results indicated that difference between the fit shown in Figure 11 and with those calibrated after every increment was not significant. In essence, the inverse analysis performed after the first construction stage "recalibrated" the model parameters in such a way that the main behavior of the soil layers could be accurately predicted throughout construction.

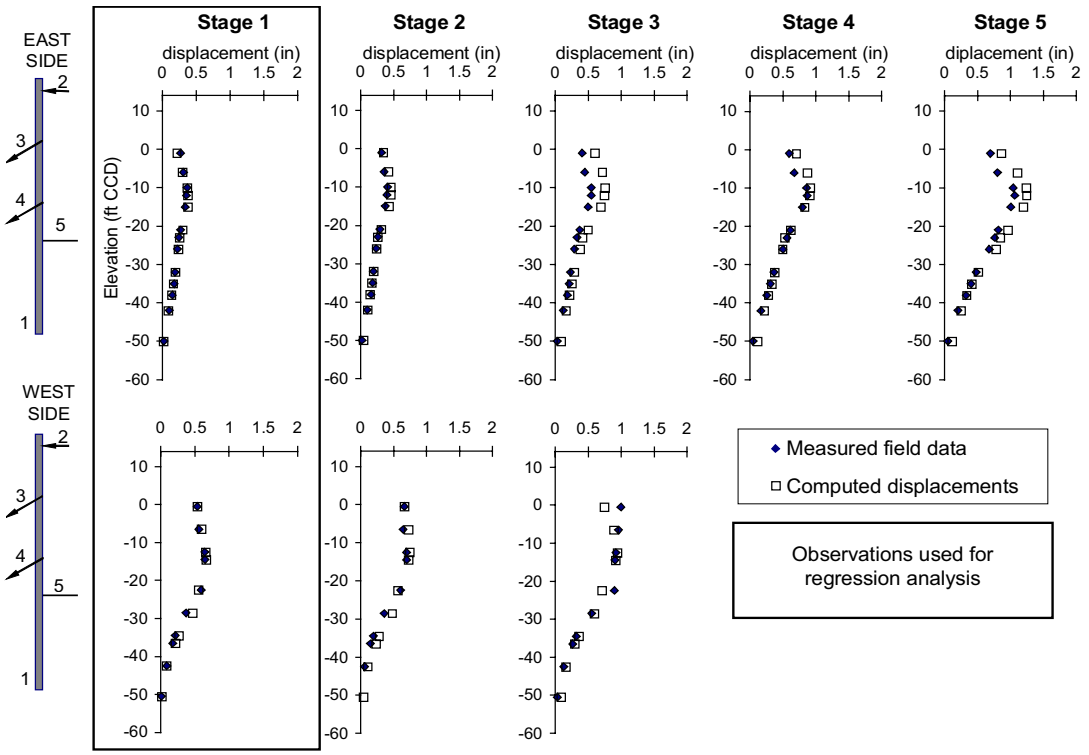

Figure 14. Comparison of observed and computed horizontal displacements (after Finno and Calvello 2005)

5.2 Applicability of Optimized Parameters in Similar Geology

To show the applicability of the optimized parameters that formed the basis of the good agreement in Figure 14 to other excavation sites in these soil deposits, the results of numerical simulations are presented in Figures 15 and 16 based on these optimized parameters for the Lurie (Finno and Roboski 2005) and the Ford Design Center (Blackburn and Finno 2007) excavations, respectively. The geologic origin of the most compressible material is similar for all three cases, but the Lurie Center is located about 2 km from the Chicago-State site and the Ford Center is located about 15 km from the site. Consequently one should expect some variability in the actual parameters at each site.

Examining the comparisons in the clay layers below EL. –5 m CCD for the Lurie data on Figure 15, reasonable agreement is observed at stages 5 and 6, with significant differences seen at stage 4. This is likely caused by the fact that the H-S model used herein does not include provisions to represent the large stiffness degradation with small strains. One must select moduli that represent the average strains within the soil mass, and when the movements are small, the average modulus should be higher in a model that does not consider the small strain modulus degradation. As noted, the agreement between computed and observed responses was good for the latter stages where the lateral movements were larger.

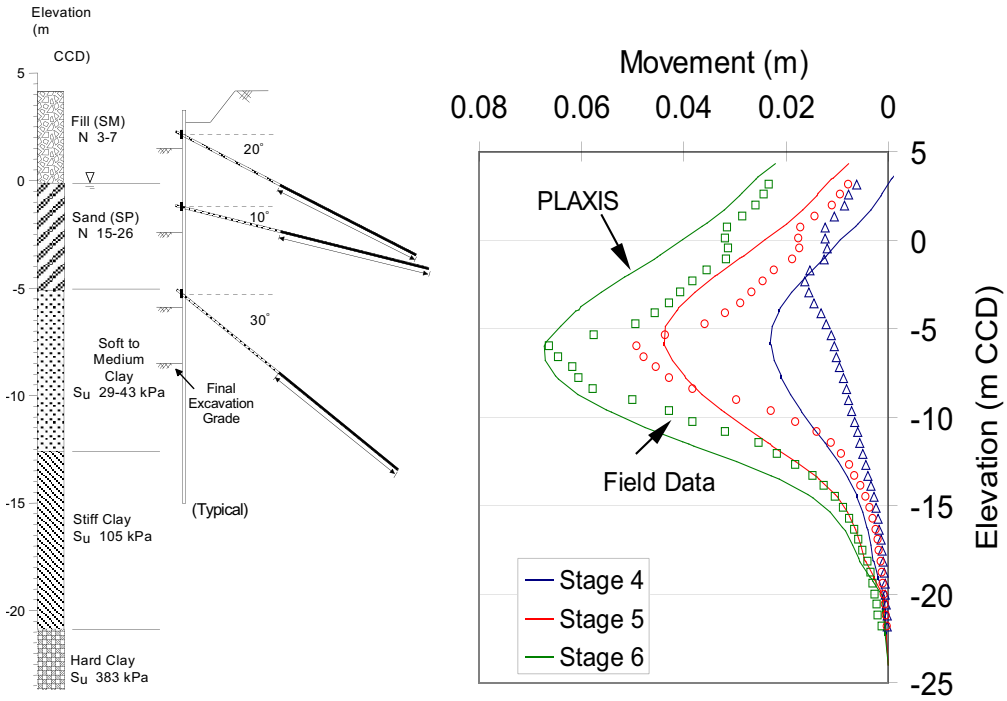

Figure 15. Computed and observed lateral movements at Lurie excavation based on optimized parameters from Chicago-State excavation

At the Ford Center, the numerical results shown in Figure 16 followed similar trends as the observed data, but with larger magnitudes. The parameters used in the analysis again were based on the larger deformations that were present at the Chicago-State site, and hence resulted in larger deformations than were observed at the Ford Center. In any case, the application of the Chicago-State based optimized parameters to both the Lurie and Ford sites resulted in reasonable agreement with the observed lateral movements, within the limitations of the analyses. Application of the inverse techniques to these data resulted in improved fit with minor changes to the parameters (Rechea 2006).

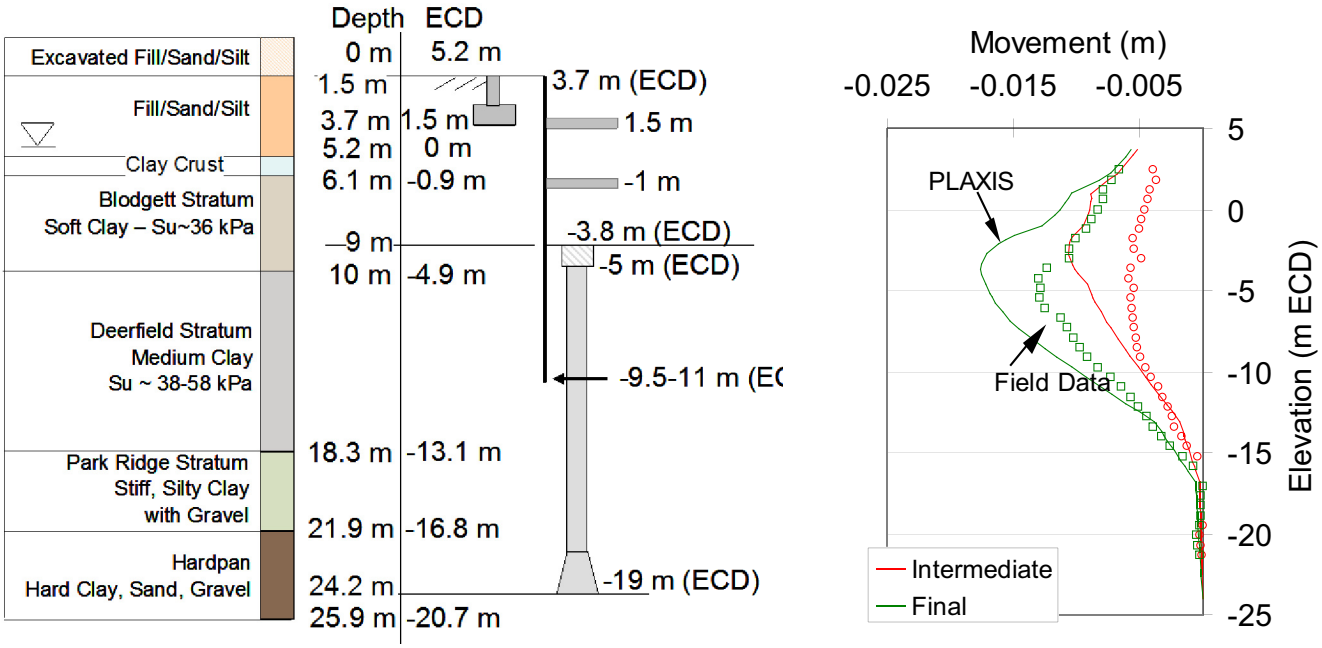

Figure 15. Computed and observed lateral movements at Ford excavation based on optimized parameters from Chicago-State excavation

6. Concluding Remarks

This paper discusses use of an adaptive management approach to control ground movements caused by making a deep supported excavation. Successful applications of this approach depend equally on reasonable numerical simulations of performance, the type of monitoring data used as observations, and the inverse analysis techniques used to minimize the difference between predictions and observed performance.

The calibration by inverse analysis of the various simulations presented herein indicated that the numerical methodology developed to optimize a finite element model of an excavation can be very effective in minimizing the errors between the measured and computed results. However, the convergence of an inverse analysis to an "optimal solution" (i.e. best-fit between computed results and observations) does not necessarily mean that the simulation is satisfactorily calibrated. A geotechnical evaluation of the optimized parameters is always necessary to verify the reliability of the solution. For a model to be considered "reliably" calibrated both the fit between computed and observed results must be satisfactory (i.e. errors are within desired and/or accepted accuracy) and the best-fit values of the model parameters must be reasonable.

The key to the successful calibration of an excavation lies in defining a "well posed" inverse analysis problem to calibrate the simulation. The parameters optimized by inverse analysis are few compared to the total number of parameters defining the behavior of the simulation. Indeed, the majority of the input parameters is estimated by conventional means and never "re-calibrated." Yet, the optimization can be extremely effective if a finite element simulation of the excavation adequately reproduces the stress history of the soil on site and the soil model adequately represented the behavior of the clays, at least in terms of appropriate field observations. In the cases presented herein with ground responses modeled by a conventional elasto-plastic soil model, the constitutive parameters that were relevant to the problem under study were calibrated based on inclinometer data obtained close to the support walls.

Acknowledgments

This work would not have been possible without the many contributions of former graduate students and post-doctoral scholars at Northwestern University who worked on developing the inverse analysis methods, collecting detailed field performance data, and conducting careful laboratory experiments, including Michele Calvello, Cecilia Rechea, Sebastian Bryson, Jill Roboski, Tanner Blackburn, Terry Holman, Wan Jei Cho, Greg Andrianis, Miltos Langousis, Young-Hoon Jung, and Taesik Kim. Financial support for this work was provided by National Science Foundation grant CMS-0219123 and the Infrastructure Technology Institute (ITI) of Northwestern University. The support of Dr. Richard Fragaszy, program director at NSF, is greatly appreciated.

References

Anandarajah A. and Agarwal D. (1991). "Computer-aided calibration of soil plasticity model." *International Journal for Numerical and Analytical Methods in Geomechanics* Vol. 15, 835-856.

Atkinson, J. H., Richardson, D., and Stallebrass, S. E. (1990). "Effect of recent stress history on the stiffness of overconsolidated soil." *Geotechnique*, 40(4), 531-540.

Arai K., Ohta H. and Kojima K. (1986). "Application of back analysis to several test embankments on soft clay deposits." *Soils and Foundations*. Vol.26(2), 60-72.

Blackburn, J.T., Sylvester, K. and Finno, R.J., "Observed bracing responses at the Ford Design Center excavation," Proceedings, 16th International Conference on Soil Mechanics and Geotechnical Engineering," Japan, 2005.

Blackburn, J.T. and Finno, R.J., (2007). "Three-Dimensional Responses Observed in an Internally Braced Excavation in Soft Clay," Journal of Geotechnical and Geoenvironmental Engineering, ASCE, 133 (11), 1364-1373.

Burland, J.B. (1989). "'Small is beautiful' – the stiffness of soils at small strains: Ninth Laurits Bjerrum Memorial Lecture." *Canadian Geotechnical Journal*, Vol. 26, 499-516.

Calisto, L. and Calebresi, G. (1998). "Mechanical behavior of a natural soft clay." *Geotechnique*, Vol. 48 (4), 495-513.

Calvello, M. (2002). “Inverse Analysis of a Supported Excavation through Chicago Glacial Clays,” PhD thesis, Northwestern University, Evanston, IL.

Calvello M. and Finno R.J. (2002). “Calibration of soil models by inverse analysis.” *Proc. International Symposium on Numerical Models in Geomechanics, NUMOG VIII*, Balkema, p. 107-116.

Calvello M. and Finno R.J. (2003). “Modeling excavations in urban areas: effects of past activities.” *Italian Geotechnical Journal*, 37(4), 9-23.

Calvello M. and Finno R.J. (2004). “Selecting parameters to optimize in model calibration by inverse analysis.” *Computers and Geotechnics*, Elsevier, Vol. 31, 5, 2004, 411-425.

Chung, C.-K. and Finno, R.J. (1992). "Influence of Depositional Processes on the Geotechnical Parameters of Chicago Glacial Clays," *Engineering Geology*, 32, 225-242.

Cho, W.J. (2007). “Recent stress history effects on compressible Chicago glacial clay,” PhD thesis, Northwestern University, Evanston, IL.

Clayton, C.R.I., and Heymann, G. (2001). “Stiffness of geomaterials at very small strains.” *Geotechnique*, Vol. 51 (3), 245-255.

Clough, G. W., Smith, E.M., and Sweeney, B.P. (1989). “Movement control of excavation support systems by iterative design.” *Current Principles and Practices, Foundation Engineering Congress,* Vol. 2, ASCE, 869-884.

Finno, R.J., “Use of monitoring data to update performance predictions of supported excavations,” theme lecture in the Proceedings, FMGM 2007, International Symposium on Field Measurements in Geomechanics, ASCE, Boston, September, 2007.

Finno, R.J., Atmatzidis, D.K., and Nerby, S.M. (1988). “Ground response to sheet-pile installation in clay," *Proceedings, Second International Conference on Case Histories in Geotechnical Engineering*, St. Louis, MO.

Finno, R.J. and Blackburn, J.T. (2005). “Automated monitoring of supported excavations,” *Proceedings, 13th Great Lakes Geotechnical and Geoenvironmental Conference, Geotechnical Applications for Transportation Infrastructure,* GPP 3, ASCE, Milwaukee, WI., 1-12.

Finno R.J., Bryson L.S. and Calvello M. (2002). “Performance of a stiff support system in soft clay.” *Journal of Geotechnical and Geoenvironmental Engineering*, ASCE, Vol. 128, No. 8, p. 660-671.

Finno, R.J. and Calvello, M. (2005). “Supported excavations: the observational method and inverse modeling.” *Journal of Geotechnical and Geoenvironmental Engineering*. ASCE, 131 (7).

Finno, R.J. and Roboski, J.F., (2005). “Three-dimensional Responses of a Tied-back Excavation through Clay,” Journal of Geotechnical and Geoenvironmental Engineering, ASCE, Vol. 131, No. 3, 273-282.

Finno, R.J. and Tu, X. (2006). “Selected Topics in Numerical Simulation of Supported Excavations,” *Numerical Modeling of Construction Processes in Geotechnical Engineering for Urban Environment,* International Conference of Construction Processes in Geotechnical Engineering for Urban Environment, Th. Triantafyllidis, ed., Bochum, Germany, Taylor & Francis, London, 3-20.

Finno, R.J., Blackburn, J.T. and Roboski, J.F., (2007). “Three-dimensional Effects for Supported Excavations in Clay,” Journal of Geotechnical and Geoenvironmental Engineering, ASCE, Vol. 133, No. 1, January, 30-36.

Ghaboussi, J. and Pecknold, D.A. (1985). “Incremental finite element analysis of geometrically altered structures.” *International Journal of Numerical Methods in Engineering*. Vol 20(11) 2061-2064.

Gens A., Ledesma A., Alonso E.E. (1996). “Estimation of parameters in geotechnical backanalysis. - 2. Application to a tunnel excavation problem.” *Computer and Geotechnics.* Vol. 18(1) pp.29-46.

Gioda, G. and Maier,G, (1980). “Direct search solution of an inverse problem in elasto-plasticity: identification of cohesion, friction angle and in situ stress by pressure tunnel tests,” *International Journal of Numerical Methods in Engineering,* Vol 15, 1823-1848.

Hashash Y.M.A., Marulanda C., Ghaboussi J. , Jung, S. (2006). “Novel approach to integration of numerical modeling and field observation for deep excavation.” *Journal of Geotechnical and Geoenvironmental Engineering*, Vol. 132(8), pp.1019-1031.

Hashash, Y.M.A., and A.J. Whittle (1996) "Ground movement prediction for deep excavations in soft clay," *Journal of Geotechnical Engineering*, Vol. 122, No. 6, 474-486.

Hill, M. (1998). “Methods and guidelines for effective model calibration.” *U.S. Geological Survey. Water-resources investigations report 98-4005*.

Holman, T.P. (2005). “Small strain behavior of compressible Chicago glacial clay.” PhD thesis, Northwestern University, Evanston, IL.

Jardine, R.J., Symes, M.J. and Burland, J.B. (1984). “The measurement of small strain stiffness in the triaxial apparatus.” *Geotechnique*, Vol. 34 (3), 323-340.

Koutsoftas, D. C., P. Frobenius, C.L Wu, D. Meyersohn, and R. Kulesza (2000). "Deformations during cut-and-cover construction of Muni Metro Turnback project," *Journal of Geotechnical and Geoenvironmental Engineering*, Vol. 126, No. 4, 344-359.

Langousis, M.. (2007). “Automated Monitoring and Inverse Analysis of a Deep Excavation in Seattle,” MS thesis, Northwestern University, Evanston, IL.

Ledesma, A., Gens, A, and Alonso, E.E. (1996). “Estimation of parameters in geotechnical backanalysis. I – Maximum likelihood approach,” *Computers and Geotechnics,* Vol. 18, No. 1, 1-27.

Levasseur S., Malécot Y., Boulon M., Flavigny E., (2007). “Soil parameter identification using a genetic algorithm.” *International Journal for Numerical and Analytical Methods in Geomechanics*, in press.

Mana, A.I. and Cough, G.W. (1981). “Prediction of movements for braced cut in clay.” *Journal of Geotechnical Engineering*, ASCE, New York, Vol. 107, No. 8, 759-777.

O’Rourke, T.D. and Clough, G.W. (1990). “Construction induced movements of insitu walls.” *Proceedings, Design and Performance of Earth Retaining Structures,* Lambe, P.C. and Hansen L.A. (eds). ASCE, 439-470.

O’Rourke, T.D. and O’Donnell, C.J. (1997). “Deep rotational stability of tiedback excavations in clay,” *Journal of Geotechnical Engineering*, ASCE, Vol. 123(6), 506-515.

Ou, C.Y., Chiou, D.C. and Wu, T.S. (1996). “Three-dimensional finite element analysis of deep excavations.” *Journal of Geotechnical Engineering*, ASCE, 122(5), 473-483.

Ou C.Y., Tang Y.G. (1994). “Soil parameter determination for deep excavation analysis by optimization.” *Journal of the Chinese Institute of Engineering*, Vol. 17(5)}, pp.671-688

Peck R.B. (1969). “Deep excavations and tunneling in soft ground.” *Proceedings, 7th International Conference of Soil mechanics and Foundation Engineering, State-of-the-ArtVolume*, 225-290.

Poeter EP and Hill M.C. (1997). “Inverse Methods: A Necessary Next Step in Groundwater Modeling,” *Ground Water*, Vol. 35, no. 2, 250-260.

Poeter E.P. and Hill M.C. (1998). “Documentation of UCODE, a computer code for universal inverse modeling.” U.S. *Geological Survey Water-Resources investigations report 98-4080*, 116 pp.

Quiñones-Rozo, C. A., Y. M. A. Hashash, and L. Y. Liu (2008). "Digital Image Reasoning for Tracking Excavation Activities," *Automation in Construction*, Vol. 17, No. 5, 608-622.

Rechea, C. (2006). “Inverse analysis of excavations in urban environments,” PhD thesis, Northwestern University, Evanston, IL.

Sakurai S. and Takeuchi K. (1983). “Back analysis of measured displacements of tunnels,” *Rock mechanics and rock engineering,* Vol.16, 173-180.

Santagata, M., Germaine, J.T. and Ladd, C.C. (2005). “Factors Affecting the Initial Stiffness of Cohesive Soils.” *Journal of Geotechnical and Geoenvironmental Engineering*, ASCE, Vol. 131(4), 430-441.

Sabatini, P.J. (1991). “Sheet-pile installation effects on computed ground response for braced excavations in soft to medium clays.” MS thesis, Northwestern University, Evanston, IL.

Schantz, T., Vermeer, P.A. and Bonnier, P.G. 1999. “Formulation and verification of the Hardening–Soil Model.” *R.B.J. Brinkgreve, Beyond 2000 in Computational Geotechnics.* Balkema, Rotterdam, 281-290.

Stallebrass, S.E. and Taylor, R.N. (1997). “The development and evaluation of a constitutive model for the prediction of ground movements in overconsolidated clay.” *Geotechnique*, Vol. 47 (2) 235-253.

Su, Y.Y., Hashash, Y.M.A. and Liu, L.Y. (2006). "Integration of construction as-built data with geotechnical monitoring of urban excavation," *Journal of Construction Engineering and Management*, Vol. 132, No. 12, 1234-1241.

Trupp, T., Marulanda, C., Hashash, Y.M.A., Liu, L., and Ghaboussi, J., (2004). Novel methodologies for tracking construction progress of deep excavations. in Geo-Trans 2004. Los Angeles, CA.

Tu, X.X. (2007). “Tangent stiffness model for clays including small strain non-linearity.” PhD thesis, Northwestern University, Evanston, IL.

Viggiani, G. and Tamagnini, C. (1999). "Hypoplasticity for modeling soil non-linearity in excavation problems." *Pre-failure Deformation Characteristics of Geomaterials*, M. Jamiolkowski, M, Lancellotta, R. and Lo Presti, D. (eds.), Balkema, Rotterdam, 581-588.

Wakita, E. and Matsuo, M. (1994). "Observational design method for earth structures constructed on soft ground." *Géotechnique*. 44, No. 4, 747-755.

Whittle, A.J. and Kavvadas, M.J. (1994). "Formulation of MIT-E3 constitutive model for overconsolidated clays." *Journal of Geotechnical and Geoenvironmental Engineering*, ASCE, Vol. 120(1), 173-198.

Whittle, A.J., Y.M.A. Hashash, and R.V. Whitman (1993). "Analysis of deep excavation in Boston," *Journal of Geotechnical Engineering*, Vol. 119, No. 1, 69-90.

Yamagami T., Jiang J.C., Ueta, Y. (1997). "Back calculation of strength parameters for landslide control works using neural networks." *Proceedings of the 9th Int. Conf. on Computer Methods and Advances in Geomechanics*, Wuhan, China.